

Super-Aligned Carbon Nanotube Films as Current Collectors for Lightweight and Flexible Lithium Ion Batteries

Ke Wang, Shu Luo, Yang Wu, Xingfeng He, Fei Zhao, Jiaping Wang,* Kaili Jiang, and Shoushan Fan

Carbon nanotube (CNT) current collectors with excellent flexibility, extremely low density (0.04 mg cm^{-2}), and tunable thickness are fabricated by cross-stacking continuous CNT films drawn from super-aligned CNT arrays.

Compared with metal current collectors, better wetting, stronger adhesion, greater mechanical durability, and lower contact resistance are demonstrated at the electrode/CNT interface. Electrodes with CNT current collectors show improvements in cycling stability, rate capability, and gravimetric energy density over those with metal current collectors. These results suggest that CNT films can function as a promising type of current collector for lightweight and flexible lithium ion batteries with high energy density.

1. Introduction

The development of soft and portable electronic devices, such as roll-up displays, smart cards, wireless sensors, and wearable devices requires flexible, lightweight, and compact lithium ion batteries (LIBs) with a high energy density, long cycle life, and excellent rate capability.^[1–3] The current collector, as a necessary component to mechanically hold the electrode material and to conduct electricity between the electrode material and the electrode lead, would substantially influence the overall performance of LIBs. Three issues regarding the current collectors need to be addressed: heavy weight; weak adhesion to the electrode material; and long-term degradation. First of all, current collectors of commercial LIBs are made of metals such as Al and Cu foils. These metal current collectors have no contribution to the overall capacity, but account for 15% and 50% of the total masses of the cathodes and anodes respectively;^[4] this would reduce the energy densities of LIBs severely. Secondly, these metal current collectors often exhibit weak adhesion and limited contact area to the electrode material. As a result, gaps associated with volumetric change during the charge and discharge

processes will occur at the electrode/current collector interface, resulting in capacity loss or poor performance at high rates. This problem will become more serious in flexible batteries, where detachments of electrode materials from current collectors are very likely to take place upon bending or folding. Thirdly, metal current collectors are susceptible to long-term exposure to corrosive chemicals. Degradation resulting from localized pitting corrosion in Al and environmentally assisted cracking in Cu was observed, which may increase the internal impedance, passivate the active electrode material, and cause

capacity and rate capability losses.^[5,6]

There have been several approaches to improving the performance of the current collectors. For instance, current collectors with roughened surfaces or novel metallic nanostructures such as nanorods, nanowires, and nanoporous architectures have been developed to increase the adhesion and contact area between the electrode materials and the current collectors.^[7–13] Nevertheless, these approaches cannot essentially improve the mechanical durability against repeated deformation that commonly occurs in flexible electronic devices, and the problem of degradation still exists in such metallic current collectors. More importantly, metals are rather heavy and not beneficial for the overall energy density of the battery. In comparison with metals, carbon materials show much lower density and better chemical stability. A variety of carbon current collectors such as graphite sheets, carbon fiber mats, carbon paper, and buckypaper, with high specific surface areas, have been developed to improve the cycle stability and gravimetric energy density.^[14–21] These carbon-based current collectors still hold rather large volumes because of their disordered microstructures and low packing density, and do not show obvious advantages in terms of the volumetric energy density. In some studies, the volumetric energy densities of LIBs with carbon current collectors were even lower than those with commercial metal current collectors.^[22] Therefore, it is critical to develop a novel type of current collector that is lightweight, thin, mechanically durable, and chemically stable for use in the next-generation flexible LIBs.

In this work, we demonstrate lightweight, thin, and flexible current collectors for LIBs based on superaligned carbon nanotube (SACNT) films drawn from SACNT arrays.^[23–26] Flexible and free-standing electrodes on CNT current collectors were

K. Wang, S. Luo, Dr. Y. Wu, X. F. He, F. Zhao,
Prof. J. P. Wang, Prof. K. L. Jiang, Prof. S. S. Fan
Department of Physics and Tsinghua-Foxconn
Nanotechnology Research Center
Tsinghua University
Beijing 100084, P. R. China
E-mail: jpwang@tsinghua.edu.cn



DOI: 10.1002/adfm.201202412

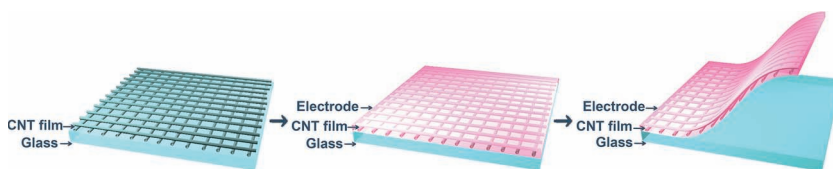


Figure 1. Schematic of the procedure for making flexible electrodes with SACNT films functioning as lightweight and thin current collectors. The SACNT sheets are cross-stacked on a glass substrate; the electrode slurry is coated on top of the CNT film; the electrode with the CNT current collector can be then easily separated from the glass substrate after drying.

fabricated by coating cross-stacked CNT films with an electrode slurry (Figure 1). There are several advantages of using SACNT films as current collectors for flexible LIBs: 1) The SACNT films are extremely lightweight and thin with an areal density of as low as 0.04 mg cm^{-2} and a thickness of less than $1 \mu\text{m}$, compared with 16 mg cm^{-2} and $20 \mu\text{m}$ for a Cu foil. Therefore higher gravimetric and volumetric energy densities of the electrodes can be expected. Specifically, the graphite-CNT electrodes exhibit more than 180% improvement in gravimetric energy density compared with the traditional graphite-Cu electrodes. 2) The porous structure of SACNT films enables easier slurry infiltration, larger contact area, better wetting, stronger adhesion, and lower contact resistance at the electrode/CNT interface. SACNT films themselves are flexible and strong enough for the structural integrity of the electrodes. Accordingly, any volumetric changes of the electrodes during electrochemical reaction and repeated mechanical deformation in flexible LIBs can be better accommodated, leading to better cycling stability, rate capability, and mechanical durability. 3) SACNT films are much more chemically stable than metal current collectors; therefore, long-term stability of LIBs with CNT current collectors is expected. 4) Fabrication of SACNT films has been scaled up to meet the industrial requirements,^[26] and mass production

of lightweight and flexible LIBs with CNT current collectors is potentially feasible.

2. Results and Discussion

2.1. Microstructures of the Graphite-CNT and Graphite-Cu Electrodes

The SACNTs used in this work had a tube diameter of $\approx 20\text{--}30 \text{ nm}$ and a length of $300 \mu\text{m}$, and possessed a high purity, clean surfaces, and strong interaction among the tubes.^[23–26] Continuous SACNT films can be directly drawn from SACNT arrays by an end-to-end joining mechanism,^[24,26,27] and their various applications such as TEM grids, loudspeakers, and touch screens, etc. have been demonstrated.^[26–32] In this work, we demonstrate a novel function of SACNT films as lightweight and thin current collectors for flexible LIBs. Figure 1 illustrates the procedure for making flexible electrodes with CNT current collectors. Continuous SACNT sheets were cross-stacked on a glass substrate to serve as a lightweight current collector to replace the traditional metal foils. The electrode slurry was then coated on top of the CNT film. After drying, a flexible and free-standing electrode with a CNT current collector could be easily separated from the glass substrate. The same electrode slurry was also coated onto a Cu foil for comparison.

The photograph in Figure 2a shows a highly flexible and free-standing graphite-CNT electrode. Upon folding, the graphite layer still adhered well with the CNT film. In comparison, the photograph of the graphite-Cu electrode in Figure 2b shows that the graphite layer detached from the Cu foil upon folding, suggesting much weaker interface adhesion than that for the graphite-CNT electrode. The greater mechanical durability

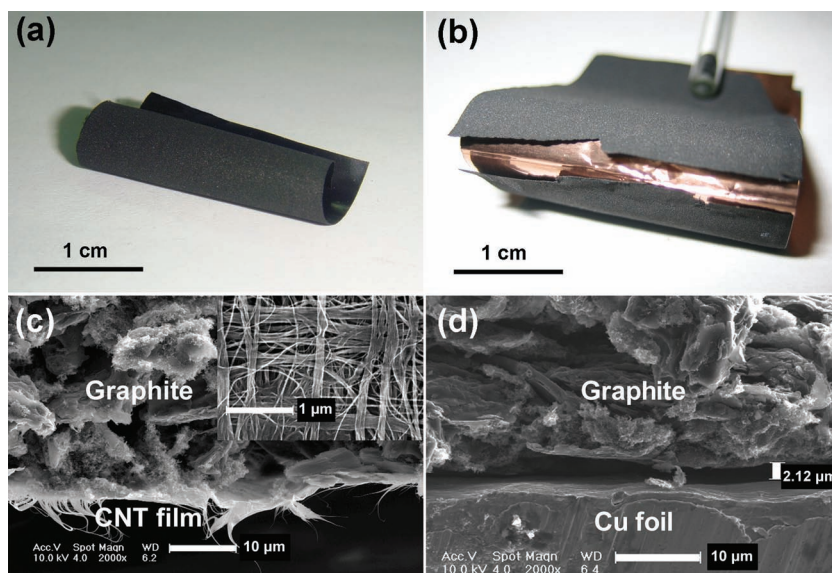


Figure 2. Photographs of: a) a freestanding and highly flexible graphite electrode with a lightweight CNT current collector, and b) a graphite-Cu electrode with the graphite layer detached from the Cu foil upon folding. Cross-sectional SEM images of graphite electrodes with: c) a thin CNT current collector, illustrating close contact at the graphite/CNT interface (the inset SEM image of the top surface of a CNT current collector shows the cross-stacked alignment and porous structure in the CNT film), and d) a thick Cu current collector, showing a $2 \mu\text{m}$ -thick gap at the graphite/Cu interface.

of the graphite-CNT electrodes is very essential for LIBs in a range of flexible electronic products. An SEM image of the top surface of a CNT film above a graphite layer is shown in the inset of Figure 2c. The CNT film remained in its original cross-stacked alignment and network structure after the slurry was coated on it. Cross-sectional SEM images of the graphite-CNT and graphite-Cu electrodes are shown in Figure 2c,d. The thicknesses of the graphite layer, CNT film, and Cu foil were 88 μm , <1 μm , and 20 μm , respectively. The small thickness of the CNT film strongly suggests that the volume occupied by the CNT current collector in the graphite-CNT electrode was almost negligible, which may lead to a high volumetric energy density of the battery. This advantage can be preserved even when more layers of CNT sheets are required to satisfy requirements of higher conductivity or mechanical properties. For instance, the thickness of 100 layers of CNT sheets is only $\approx 4\text{--}5\ \mu\text{m}$. Close contact at the graphite/CNT interface was observed, while an appreciable gap of around 2 μm remained at the graphite/Cu interface.

Such distinct interface phenomena could be attributed to the different morphologies of these two kinds of current collectors. The CNT film is highly porous as shown in Figure 2c, and therefore the graphite slurry can easily infiltrate into the spaces among the individual tubes, leading to an increased interfacial contact area between the graphite layer and the CNT current collector. On the contrary, the Cu foil is relatively flat and smooth that makes the slurry adhesion more difficult, and the interfacial contact area between the active materials and the Cu foil is rather limited.

2.2. Wetting and Adhesion Properties at the Graphite/CNT and Graphite/Cu Interfaces

The wetting properties at the graphite/CNT and graphite/Cu interfaces were investigated. Figure 3a,b show photographs of graphite slurry droplets (15 μL) on a cross-stacked SACNT film and a Cu foil, respectively. The contact angle at the graphite/CNT interface (19°) was much smaller than that at the graphite/Cu interface (48°). The graphite slurry expanded on the CNT film to a further extent (6.7 mm in diameter) than on the Cu foil (5.7 mm in diameter). These results indicate a smaller surface tension at the graphite/CNT interface. It is the porous nature of the CNT film and the better wetting at the graphite/CNT interface that result in the closer contact between the graphite layer and the CNT current collector, suggesting stronger adhesion at the graphite/CNT interface compared with that at the graphite/Cu interface.

The interface adhesion of the graphite-CNT and graphite-Cu electrodes was further characterized by single-lap shear tests and their shear strengths are illustrated in Figure 4a. The shear strength of the graphite-CNT electrode was 0.12 MPa. Fracture surfaces of the graphite-CNT electrode are shown in Figure 4b and the active graphite materials can be observed on both sides. These results suggest that the graphite-CNT electrode fractured within the graphite layer and the interfacial bonding at the graphite/CNT interface was stronger than the graphite layer itself. On the contrary, fracture surfaces of the graphite-Cu electrode in Figure 4b show that most part of the graphite

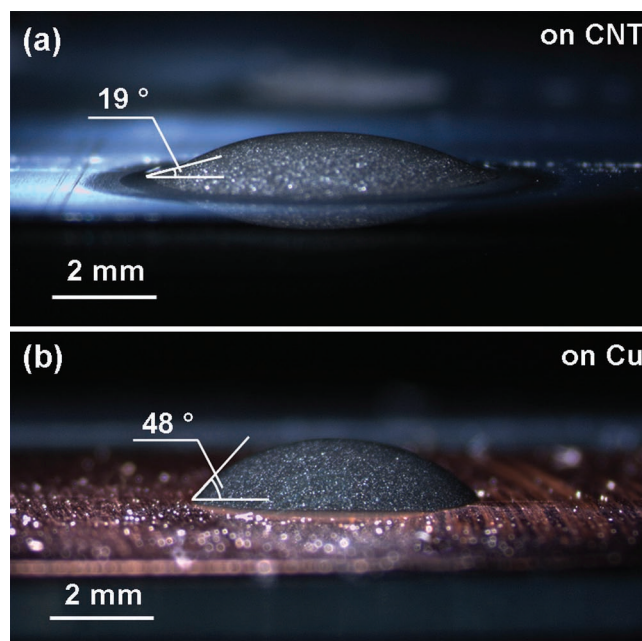


Figure 3. Photographs of graphite slurry droplets (15 μL) on: a) a porous CNT film, and b) a flat Cu foil. The smaller contact angle and the larger droplet diameter on the CNT film reveal better wetting and easier slurry infiltration at the graphite/CNT interface than at the graphite/Cu interface.

layer detached from the Cu foil. The graphite-Cu electrode actually failed at the rather weak graphite-Cu interface with a shear strength of as low as 0.04 MPa. The results of the interfacial shear tests show good agreement with the cross-sectional SEM observation and the contact angle measurements, further verifying the better wetting and stronger adhesion at the graphite-CNT interface. With the excellent interface properties, tight contact between the CNT films and graphite layer will be maintained upon any volumetric change during cycling even at large currents. Therefore excellent cycle stability and rate capability of the graphite-CNT electrodes can be expected.

2.3. SACNT Films as Both Current Collectors and Mechanical Supports

SACNT films serve as lightweight and thin current collectors for LIBs due to their high electrical conductivity. The sheet resistance of a single-layer of pristine SACNT film is around 1000 Ω per sq. It should be noted that this value is higher than that of the conventional metal current collectors. However, by stacking a number of CNT sheets together, the sheet resistance of the SACNT film can be decreased dramatically. For instance, as the number of CNT layers increased to 20 and 100, the sheet resistance of the SACNT films decreased to 66 Ω per sq. and 11 Ω per sq., respectively. SACNT films with such a low resistance can function well as conductive substrates for electron transfer in LIBs. The number of CNT layers and the thickness and conductivity of the CNT current collectors can be further optimized for specific systems and applications.

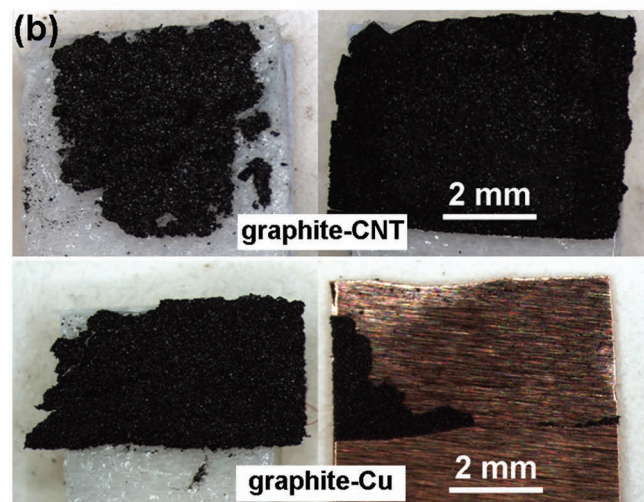
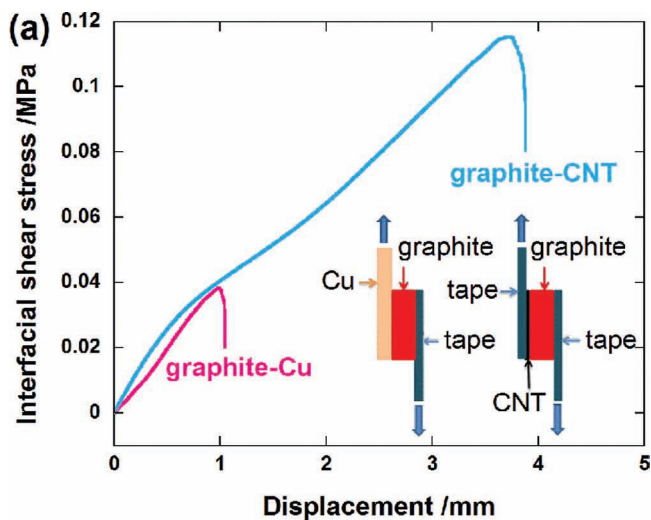


Figure 4. a) Setup for the single-lap shear tests and the interfacial shear test results of the graphite-CNT and graphite-Cu electrodes. b) Fracture surfaces of the graphite-CNT and graphite-Cu electrodes. The graphite-CNT electrode fractured within the graphite layer and the graphite-Cu electrode failed at the weak graphite-Cu interface, demonstrating stronger adhesion at the graphite-CNT interface.

In addition, due to the excellent mechanical properties of SACNTs, they can also provide structural support for the electrodes.^[33] Tensile stress–strain curves of the graphite sheets with and without the CNT current collector are shown in **Figure 5**. The free-standing graphite sheet alone was very weak with a Young's modulus and a tensile strength of only 11 MPa and 0.08 MPa, respectively. For comparison, the graphite sheet with the CNT current collector was much stronger with a Young's modulus and a tensile strength of 117 MPa and 1.08 MPa, respectively, corresponding to about 10-times improvement. These results reveal that the CNT current collector works well as a mechanical support and provides structural integrity to the electrode, potentially to cushion any volume change of the electrode on cycling and to obtain a long cycle life.

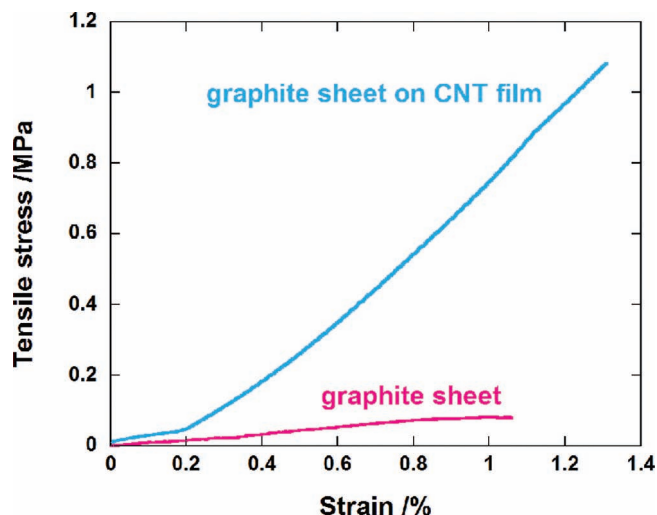


Figure 5. Tensile stress–strain curves of graphite sheets with and without the CNT current collector that functions as a mechanical support for the graphite electrode.

2.4. Electrochemical Properties of the Graphite-CNT and Graphite-Cu Electrodes

The initial charge and discharge profiles of the graphite-CNT and graphite-Cu electrodes at 0.1C (weight of graphite: 3.0–4.5 mg, current: 0.11–0.17 mA) are shown in **Figure 6**. Both electrodes feature similar plateaus of graphite at around 0.1 V. Such similarity indicates that there was not any additional electrochemical reaction involved when the novel type of SACNT current collector was introduced. The graphite-CNT electrode delivered a larger initial capacity than the graphite-Cu electrode, which can be ascribed to the excellent graphite/CNT interface properties and more sufficient utilization of the active material. The cycling performances of these electrodes

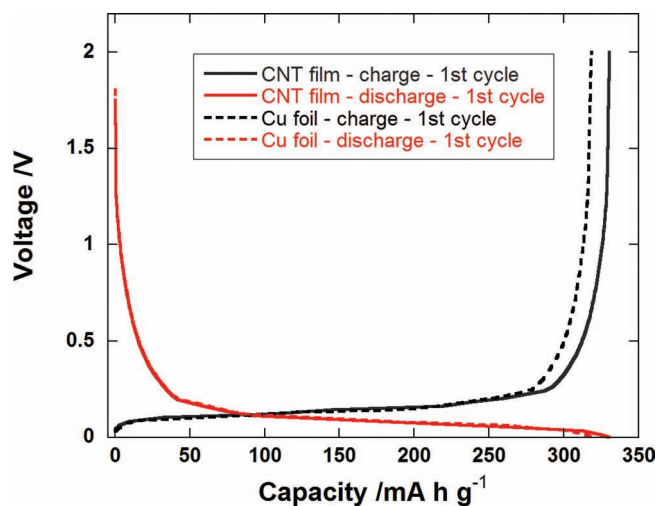


Figure 6. Initial charge-discharge profiles of the graphite-CNT and graphite-Cu electrodes at 0.1C.

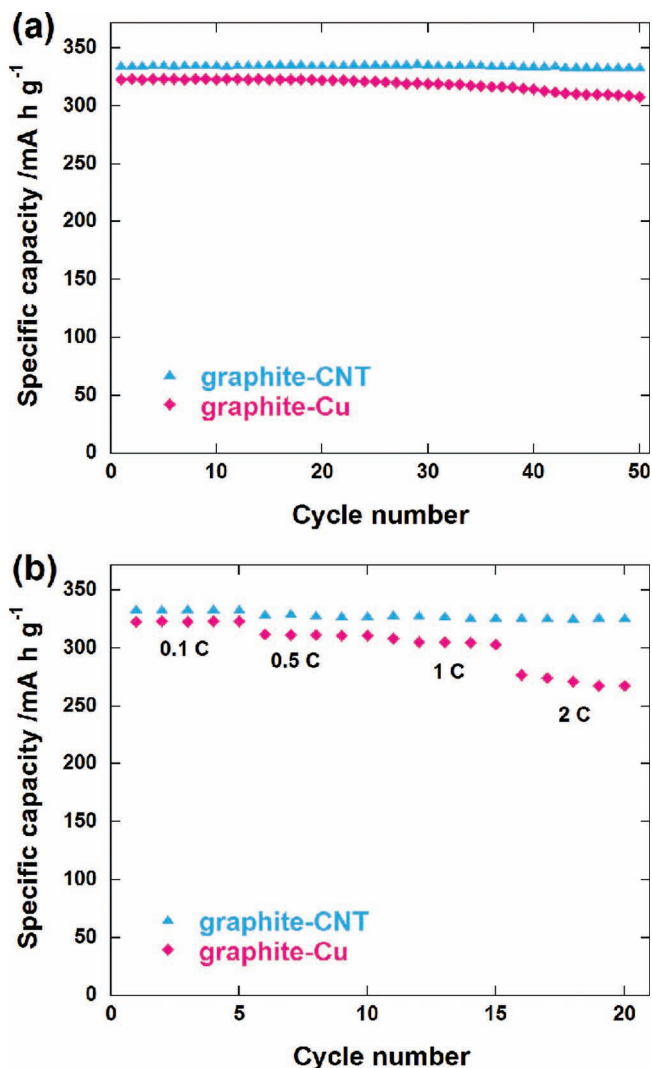


Figure 7. a) Cycling (0.1C) and b) rate performances of the graphite-CNT and graphite-Cu electrodes, revealing the superior electrochemical properties of the graphite-CNT electrodes.

at 0.1C are shown in **Figure 7a**. The graphite-CNT electrode showed excellent cycling stability with a specific capacity (based on the mass of the active graphite material) of 335 mA h g⁻¹ at 0.1C and a capacity retention of 99.1% after 50 cycles, while

the graphite-Cu electrodes displayed slightly inferior cycling performance with a specific capacity of 318 mA h g⁻¹ at 0.1C and a capacity retention of 96.2% after 50 cycles. The rate performances of the graphite-CNT and graphite-Cu electrodes are shown in **Figure 7b**. The graphite-CNT electrodes exhibited much superior rate capability than the graphite-Cu electrodes. The graphite-CNT electrodes showed a capacity of 326 mA h g⁻¹ at 2C, corresponding to 97.3% of the capacity at 0.1C, while the graphite-Cu electrodes showed a capacity of only 271 mA h g⁻¹ at 2C, corresponding to only 85.2% of the capacity at 0.1C. The graphite-CNT electrodes in this work exhibited much better rate performance than other carbon based electrodes with various kinds of current collector reported in the literature,^[14,34–36] as listed in **Table 1**. For example, graphite electrodes with Cu current collectors demonstrated a capacity retention of only 35% compared with the capacity at 0.1C.^[14] For mesocarbon microbead-Cu electrodes, the capacity retentions were 66% and 88% in previous studies.^[34,35]

It is interesting to determine the internal resistance of the graphite-Cu and graphite-CNT electrodes to interpret the difference in their specific capacities, particularly at high rates. The magnitude of internal resistance can be characterized by the voltage drop, or *IR* drop, when charging or discharging is switched to discharging or charging (**Figure 8**). The electrode with a CNT current collector exhibited a larger *IR* drop (0.25 V) compared with the electrode coated on a Cu foil (0.20 V) at the initial cycle at 0.1C because of the higher intrinsic resistance of the CNT film. The difference in *IR* drop was reduced as the electrodes were charged and discharged repeatedly. After 50 cycles, the *IR* drop of both two electrodes decreased to around 0.10 V. The decrease of the *IR* drop could probably stem from slow wetting of the electrode by the electrolyte or the gradual stabilization of the solid electrolyte interface. The intrinsic resistance of these two types of current collectors can be considered as unchanged upon cycling; therefore, the same *IR* drop after repeated charging and discharging cycles may indicate a lower contact resistance between the graphite electrode and the CNT current collector. Such a phenomenon might be ascribed to the better wetting and larger contact area at the graphite/CNT interface, which can provide more charge transfer pathways. Moreover, the superiority of the graphite-CNT electrode becomes more pronounced after consecutive cycles at various high rates. As the rates increased to 1C and 2C, the *IR* drop of the graphite-Cu electrode increased much faster than that of the graphite-CNT electrode. The *IR* drops

Table 1. Rate performances of carbon-based electrodes with various types of current collector.

Sample description	Capacity at low rate [mAh g ⁻¹]	Capacity at high rate [mAh g ⁻¹]	Capacity retention (high rate capacity/low rate capacity)	Reference
Graphite on a CNT film	335 (0.1C)	326 (2C)	97%	This work
Graphite on a Cu foil	318 (0.1C)	271 (2C)	85%	This work
Graphite on a Cu foil	370 (0.1C)	130 (2C)	35%	Yazici et al. ^[14]
Mesocarbon microbead on a Cu foil	300 (0.2C)	200 (1C)	66%	Dileo et al. ^[34]
Mesocarbon microbead on a Cu foil	340 (0.2C)	300 (2C)	88%	Hossain et al. ^[35]
Buckypaper as both anode and current collector	220 (0.1C)	200 (2C)	90%	Chew et al. ^[36]
		175 (10C)	80%	

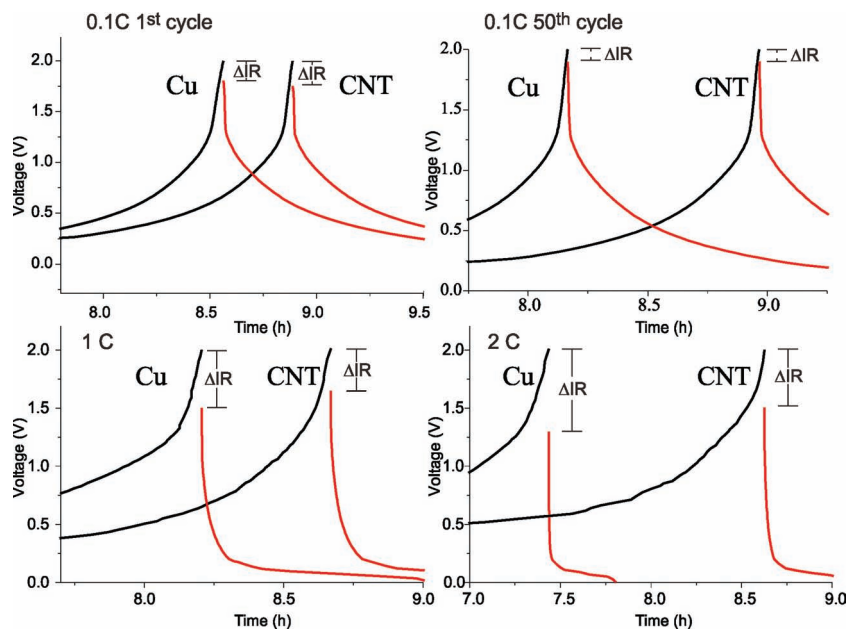


Figure 8. IR-drop data of the graphite-CNT and graphite-Cu electrodes at different rates when charging is switched to discharging. Top left: initial cycle at 0.1C. Top right: 50th cycle at 0.1C. Bottom left: initial cycle at 1C. Bottom right: initial cycle at 2C. Note, to better elucidate, only parts of the curves are presented.

of the graphite-CNT electrode and graphite-Cu electrode were 0.35 V and 0.50 V at 1C, and increased to 0.49 V and 0.70 V at 2C. The pronounced difference in IR drops at high rate suggests that more serious local polarization occurred within the graphite-Cu electrode at large currents. Bonded with weak van der Waals forces, the spacing between graphene layers in the graphite structure will change during the lithiation and delithiation processes. The volume change of the graphite electrode will occur more quickly at high rates. Because of the weak adhesion between the graphite layer and the Cu foil, microgaps associated with such volume change will be generated at the graphite/Cu interface, leading to significant increase in the contact resistance at high rates. This contact issue becomes an obstacle to charge transfer and overshadows the low intrinsic resistance of the Cu foil, resulting in more serious polarization, insufficient utilization of the active material, and poor rate performance of the graphite-Cu electrode. On the contrary, we have demonstrated the flexibility and porous structure of the SACNT films, together with the strong adhesion at the graphite/CNT interface. With these characteristics, CNT current collectors made from SACNT films can be an efficient cushion for such volumetric changes, and tight contact and efficient electron transfer will be maintained at the graphite/CNT interface. The analysis of the IR drop data of the graphite-Cu and graphite-CNT electrodes suggests lower contact resistance at the graphite/CNT interface and strongly supports the superiority of SACNT films as a novel kind of current collectors for high performance LIBs. In this study, graphite was used as the anode material. When some other active materials with poorer conductivity, such as LiFePO_4 and $\text{Li}_4\text{Ti}_5\text{O}_{12}$, are used, the overall improvement in the conductivity and high rate performance could be even more significant for the CNT current collector. It is also expected

that this type of CNT current collector can be used as a promising choice for electrodes that utilize alloying mechanisms associated with large volume changes (e.g., Si).

2.5. Energy Densities of the Electrodes with CNT and Metal Current Collectors

Because the CNT current collector is extremely lightweight and thin, electrodes with CNT current collectors display much higher gravimetric and volumetric energy densities (based on the total mass and volume of the electrode material layer and the current collector) than electrodes with metal current collectors. Considering the low areal density of a single layer of SACNT film at only $2 \times 10^{-3} \text{ mg cm}^{-2}$, the areal density of a CNT current collector consisting of 20 layers of cross-stacked CNT films is as low as 0.04 mg cm^{-2} , while the areal density of a Cu foil with a thickness of $20 \mu\text{m}$ is 16 mg cm^{-2} , which is 400 times heavier than the CNT current collector. As a result, the gravimetric energy densities (based on the total mass of the graphite layer and the current collector) of the graphite-CNT electrodes were much higher than those of the graphite-Cu electrodes. As shown in Figure 9a, when the thickness of the graphite layer was $88 \mu\text{m}$, the energy density of the graphite-CNT electrode was as high as 54.3 W h kg^{-1} , showing more than 180% improvement than the graphite-Cu electrode (18.9 W h kg^{-1}). The graphite-CNT electrode also exhibited a high volumetric energy density (based on the total volume of the graphite layer and the current collector) of 60.9 W h L^{-1} , which is more than 30% increase than the graphite-Cu electrode. Furthermore, the advantage in energy densities of the graphite-CNT electrodes will become even more significant for thinner electrodes. According to the calculated results, as the thickness of the graphite layer decreases to $10 \mu\text{m}$, the graphite-CNT electrode can show more than 1580% and 219% improvements in gravimetric and volumetric energy densities respectively, compared with the graphite-Cu electrode.

The CNT current collectors can be used with other electrode materials as well, such as $\text{Li}_4\text{Ti}_5\text{O}_{12}$ and LiCoO_2 , and much higher energy densities can be achieved. As shown in Figure 9b, when the thickness of the LiCoO_2 layer was $57 \mu\text{m}$, the energy density of the LiCoO_2 -CNT electrode was as high as 478 W h kg^{-1} , showing more than 53% improvement than the LiCoO_2 -Al electrode (312 W h kg^{-1}). These results reveal that the SACNT films can serve as lightweight and thin current collectors for both cathodes and anodes, leading to LIBs with high gravimetric and volumetric energy densities. Since metal current collectors account for 15–25% of the total mass of the traditional batteries,^[4] the gravimetric energy density of the whole cell can be increased by at least 15% by replacing the metal current collectors with SACNT films. Considering future portable and flexible electronics calls for much thinner energy devices, it is promising to use SACNT films as lightweight, thin, and

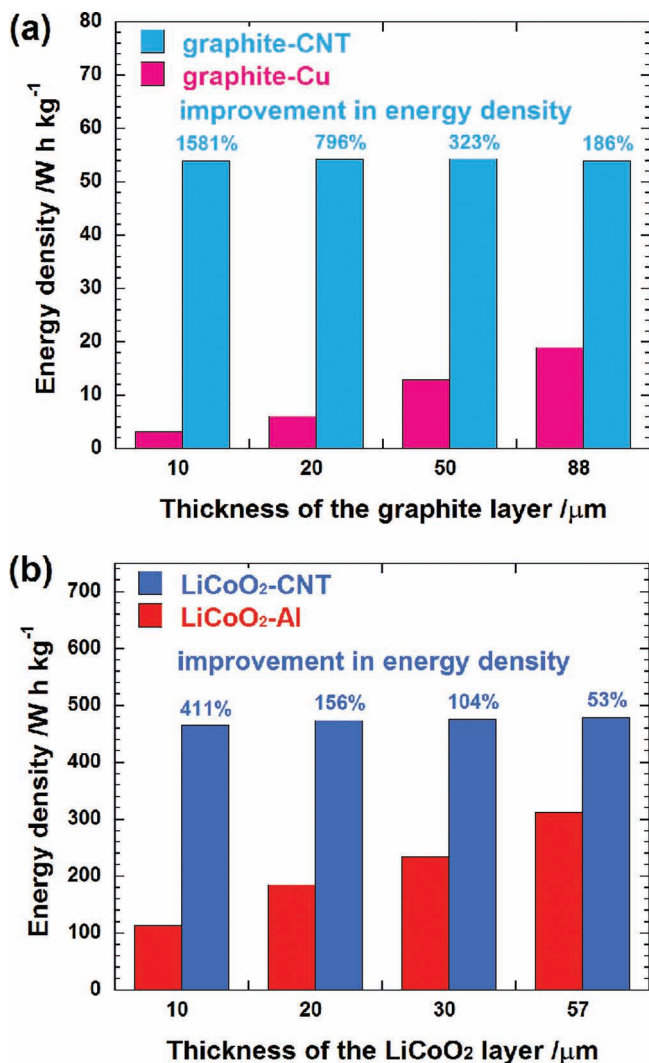


Figure 9. Energy densities (based on the total mass of the electrode material layer and the current collector) of: a) the graphite-CNT and graphite-Cu electrodes, and b) the LiCoO₂-CNT and LiCoO₂-Al electrodes. Much higher energy densities were achieved in the electrodes with the lightweight CNT current collectors.

durable current collectors for flexible LIBs with high energy density.

3. Conclusions

In conclusion, we developed a novel type of lightweight, thin, and flexible CNT current collector to replace the widely used heavy metal current collectors for LIBs. The CNT current collectors with tunable thickness functioned as a mechanical support for the structural integrity and enabled excellent mechanical durability and efficient electron transfer at the electrode/CNT interface. As a result, the graphite-CNT electrodes displayed outstanding cycling stability (335 mA h g⁻¹ at 0.1C with a capacity retention of 99.1% after 50 cycles) and rate

capability (326 mA h g⁻¹ at 2C, showing 20.3% improvement than the graphite-Cu electrodes). By comparing the IR drop data of electrodes with CNT and Cu current collectors at various rates, it can be concluded that the graphite/CNT interface displayed lower contact resistance compared with the graphite/Cu interface, leading to a much better performance upon long term cycling or at large currents. The extremely light weight of the CNT film in the graphite-CNT electrodes resulted in more than 180% improvement in gravimetric energy density than the graphite-Cu electrodes. Such superior CNT current collectors can be used with a variety of electrode materials. Based on the fact that the fabrication of SACNT films has been scaled up, we can expect that the mass production of flexible LIBs with high energy density using SACNT current collectors is potentially feasible.

4. Experimental Section

Fabrication of CNT Films: SACNT arrays with a tube diameter of $\approx 20\text{--}30$ nm and a height of 300 μm were synthesized on 8-inch silicon wafers by chemical vapor deposition (CVD) with iron as the catalyst and acetylene as the precursor. Details of the synthesis procedure can be found in previous papers.^[23–26] Continuous SACNT films can be directly drawn from SACNT arrays by an end-to-end joining mechanism.^[24,26,27]

Fabrication of Electrodes with CNT and Metal Current Collectors: 20 layers of SACNT films were first cross-stacked onto a glass substrate for use as a current collector. The electrode slurry was prepared by mixing graphite (20 μm in diameter, Changsha Xingcheng Microlite Graphite Co., China) or LiCoO₂ (10 μm in diameter, Reshine, China), carbon black (Super-P, 50 nm in diameter, Timcal Ltd., Switzerland), and poly(vinylidene difluoride) (PVDF) in *N*-methyl-2-pyrrolidone (NMP) solvent at a weight ratio of 8:1:1. The electrode slurry was coated on top of the SACNT current collector. After drying, flexible and free-standing graphite-CNT electrodes or LiCoO₂-CNT electrodes could be easily separated from the glass substrate. The same electrode slurry was also coated onto a Cu foil or an Al foil for comparison. These electrode sheets were punched into circular discs with a diameter of 10 mm and dried at 120 °C for 24 h in a vacuum oven. The weights of graphite and LiCoO₂ in each disc were around 3–4.5 mg and 4.5–6.0 mg, respectively.

Characterization: The sheet resistances of the CNT films were measured using a four-point method using a ResMap system (Creative Design Engineering Inc., USA). The top surfaces and cross sections of the graphite-CNT and graphite-Cu electrodes were observed by scanning electron microscopy (SEM) (Sirion 200, FEI, USA). The contact angles and surface contact areas of the graphite slurry droplets on the CNT and Cu current collectors were measured using an optical microscope.

Interfacial single-lap shear tests of the graphite-CNT and graphite-Cu electrodes were performed using an Instron 5848 microtester at a strain rate of 10% min⁻¹. The setup for the single-lap shear test is shown in Figure 4a. The dimensions of the graphite layer were 5 mm \times 5 mm. Two pieces of tape were glued on both sides of the graphite-CNT electrode and then fixed in the grips. For the graphite-Cu electrode, one piece of tape was glued to the graphite layer and fixed in one grip. The part of Cu foil without any slurry coating was fixed directly in the other grip. Fracture surfaces of the graphite-CNT and graphite-Cu electrodes were observed by optical microscopy in order to study the failure mechanism. Tensile tests of the graphite sheets with and without the CNT current collector were performed using an Instron 5848 microtester at a strain rate of 1% min⁻¹.

Coin-type (CR 2016) half-cells were assembled in an argon-filled glove box (M. Braun inert gas systems Co. Ltd., Germany) with the graphite-CNT, graphite-Cu, LiCoO₂-CNT, or LiCoO₂-Al discs as the working electrodes, and Li metal as the reference electrode. A porous polymer film (Celgard 2400) was used as the separator. A 1 M LiPF₆

solution in ethylene carbonate (EC) and diethyl carbonate (DEC) mixed at a weight ratio of 1:1 was used as the electrolyte. The cells were tested using a Land battery-test system (Wuhan Land Electronic Co., China) at room temperature, with cut-off voltages of 0–2 V and 3–4.3 V for the graphite and LiCoO₂ electrodes, respectively.

Acknowledgements

This work was supported by the National Basic Research Program of China (2012CB932301) and the NSFC (51102146 and 50825201).

Received: August 23, 2012

Published online: October 19, 2012

-
- [1] J. M. Tarascon, M. Armand, *Nature* **2001**, 414, 359.
- [2] H. Nishide, K. Oyaizu, *Science* **2008**, 319, 737.
- [3] M. Armand, J. M. Tarascon, *Nature* **2008**, 451, 652.
- [4] B. A. Johnson, R. E. White, *J. Power Sources* **1998**, 70, 48.
- [5] P. Arora, R. E. White, M. Doyle, *J. Electrochem. Soc.* **1998**, 145, 3647.
- [6] J. W. Braithwaite, A. Gonzales, G. Nagasubramanian, S. J. Lucero, D. E. Peebles, J. A. Ohlhausen, W. R. Cieslak, *J. Electrochem. Soc.* **1999**, 146, 448.
- [7] L. Taberna, S. Mitra, P. Poizot, P. Simon, J. M. Tarascon, *Nat. Mater.* **2006**, 5, 567.
- [8] M. Yao, K. Okuno, T. Iwaki, M. Kato, S. Tanase, K. Emura, T. Sakai, *J. Power Sources* **2007**, 173, 545.
- [9] Y. L. Kim, Y. K. Sun, S. M. Lee, *Electrochim. Acta* **2008**, 53, 4500.
- [10] X. Y. Fan, F. S. Ke, G. Z. Wei, L. Huang, S. G. Sun, *J. Alloys Compd.* **2009**, 476, 70.
- [11] S. R. Gowda, A. L. M. Reddy, X. Zhan, H. R. Jafry, P. M. Ajayan, *Nano Lett.* **2012**, 12, 1198.
- [12] W. Xu, N. L. Canfield, D. Y. Wang, J. Xiao, Z. M. Nie, X. Li, W. D. Bennett, C. C. Bonham, J. G. Zhang, *J. Electrochem. Soc.* **2010**, 157, A765.
- [13] S. C. Zhang, Z. J. Du, R. X. Lin, T. Jiang, G. R. Liu, X. M. Wu, D. S. Weng, *Adv. Mater.* **2010**, 22, 5378.
- [14] M. S. Yazici, D. Krassowski, J. Prakash, *J. Power Sources* **2005**, 141, 171.
- [15] C. Arbizzani, M. Lazzari, M. Mastragostino, *J. Electrochem. Soc.* **2005**, 152, A289.
- [16] J. C. Guo, A. Sun, C. S. Wang, *Electrochem. Commun.* **2010**, 12, 981.
- [17] J. W. Choi, L. B. Hu, L. F. Cui, J. R. McDonough, Y. Cui, *J. Power Sources* **2010**, 195, 8311.
- [18] S. K. Martha, J. O. Kiggans, J. Nanda, N. J. Dudney, *J. Electrochem. Soc.* **2011**, 158, A1060.
- [19] L. B. Hu, H. Wu, F. La Mantia, Y. A. Yang, Y. Cui, *ACS Nano* **2010**, 4, 5843.
- [20] J. C. Lytle, J. M. Wallace, M. B. Sassin, A. J. Barrow, J. W. Long, J. L. Dysart, C. H. Renninger, M. P. Saunders, N. L. Brandell, D. R. Rolison, *Energy Environ. Sci.* **2011**, 4, 1913.
- [21] S. H. Ng, J. Wang, Z. P. Guo, G. X. Wang, H. K. Liu, *Electrochim. Acta* **2005**, 51, 23.
- [22] C. Arbizzani, S. Beninati, A. Lazzari, M. Mastragostino, *J. Power Sources* **2006**, 158, 635.
- [23] K. L. Jiang, Q. Q. Li, S. S. Fan, *Nature* **2002**, 419, 801.
- [24] X. B. Zhang, K. L. Jiang, C. Teng, P. Liu, L. Zhang, J. Kong, T. H. Zhang, Q. Q. Li, S. S. Fan, *Adv. Mater.* **2006**, 18, 1505.
- [25] K. Liu, Y. H. Sun, L. Chen, C. Feng, X. F. Feng, K. L. Jiang, Y. G. Zhao, S. S. Fan, *Nano Lett.* **2008**, 8, 700.
- [26] K. L. Jiang, J. P. Wang, Q. Q. Li, L. A. Liu, C. H. Liu, S. S. Fan, *Adv. Mater.* **2011**, 23, 1154.
- [27] K. Liu, Y. H. Sun, P. Liu, J. P. Wang, Q. Q. Li, S. S. Fan, K. L. Jiang, *Nanotechnology* **2009**, 20, 335705.
- [28] L. Zhang, C. Feng, Z. Chen, L. Liu, K. L. Jiang, Q. Q. Li, S. S. Fan, *Nano Lett.* **2008**, 8, 2564.
- [29] H. X. Zhang, C. Feng, Y. C. Zhai, K. L. Jiang, Q. Q. Li, S. S. Fan, *Adv. Mater.* **2009**, 21, 2299.
- [30] L. Xiao, Z. Chen, C. Feng, L. Liu, Z. Q. Bai, Y. Wang, L. Qian, Y. Y. Zhang, Q. Q. Li, K. L. Jiang, S. S. Fan, *Nano Lett.* **2008**, 8, 4539.
- [31] P. Liu, L. Liu, Y. Wei, K. Liu, Z. Chen, K. L. Jiang, Q. Q. Li, S. S. Fan, *Adv. Mater.* **2009**, 21, 3563.
- [32] C. Feng, K. Liu, J. S. Wu, L. Liu, J. S. Cheng, Y. Y. Zhang, Y. H. Sun, Q. Q. Li, S. S. Fan, K. L. Jiang, *Adv. Funct. Mater.* **2010**, 20, 885.
- [33] S. Luo, K. Wang, J. P. Wang, K. L. Jiang, Q. Q. Li, S. S. Fan, *Adv. Mater.* **2012**, 24, 2294.
- [34] R. A. Dileo, A. Castiglia, M. J. Ganter, R. E. Rogers, C. D. Cress, R. P. Raffaele, B. J. Landi, *ACS Nano* **2010**, 4, 6121.
- [35] S. Hossain, Y. K. Kim, Y. Saleh, R. Loutfy, *J. Power Sources* **2003**, 114, 264.
- [36] S. Y. Chew, S. H. Ng, J. Z. Wang, P. Novak, F. Krumeich, S. L. Chou, J. Chen, H. K. Liu, *Carbon* **2009**, 47, 2976.